Available online at www.scholarsresearchlibrary.com

Scholars Research Library

Der Pharmacia Lettre, 2016, 8 (4):173-185
(http://scholarsresearchlibrary.com/archive.html)

ISSN 0975-5071
USA CODEN: DPLEB4

Corrosion Inhibition of Steel in phosphoric acid by Sulfapyridine: Experimental and Theoretical Studies

L. Adardour[1,2], H. Lgaz[1, 3], R. Salghi[3*], M. Larouj[1], S. Jodeh[4,*], M. Zougagh[5,6], O. Hamed[4] and M. Taleb[2]

[1]*Laboratory Separation Processes, Faculty of Science, University IbnTofail PO Box 242, Kenitra, Morocco*
[2]*Laboratoire d'Ingénierie de Modélisation et d'Environnement, Faculté des Sciences Dhar El Mehraz FES B.P. 1796 Atlas Fès MAROC.*
[3]*Laboratory of Applied Chemistry and Environment, ENSA, UniversitéIbnZohr,PO Box 1136, 80000 Agadir, Morocco*
[4]*Department of Chemistry, An-Najah National University, P. O. Box 7, Nablus, Palestine*
[5]*Regional Institute for Applied Chemistry Research, IRICA, E-13004, Ciudad Real, Spain*
[6]*Castilla-La Mancha Science and Technology Park, E-02006, Albacete, Spain*

ABSTRACT

*The corrosion inhibition efficiency of Sulfapyridine(**SFP**) for carbon steel in 2.0 M H_3PO_4 has been studied using weight loss, polarization, electrochemical and impedance spectroscopy techniques. The results show that **SFP** is a good inhibitor in 2.0 M H_3PO_4. Effects of temperature and acid concentration on inhibitive performance were investigated. Polarization curves reveal that **SFP** acts as a mixed-type inhibitor. The electrochemical impedance spectroscopy showed that the charge transfer resistance increases and the double layer capacitance decreases on increasing Sulfapyridine concentration. Activation energy of corrosion and other thermodynamic parameters such as standard free energy, standard enthalpy, and standard entropy of the adsorption process revealed better and well-ordered physical adsorption mechanism in the presence of Sulfapyridine. Adsorption isotherms in absence or presence of **SFP** as inhibitor appropriately fit the Langmuir isotherm. Theoretical investigations have established that the interaction of **SFP** with the metal steel surface is mainly through the Nitrogen, oxygen atoms, sulphonyl group and the π system of the aromatic ring.*

Keywords: carbon steel, corrosion, H_3PO_4, Sulfapyridine, EIS, Polarization, DFT.

INTRODUCTION

Corrosion is a fundamental process playing an important role in economics and safety, particularly for metals and alloys. Steel has found wide applications in a broad spectrum of industries and machinery; despite its tendency to corrosion. Phosphoric acid (H_3PO_4) is widely used in the production of fertilizers and surface treatment of steel such as chemical and electrolytic polishing or etching, chemical coloring, removal of oxide film, phosphating, passivating, and surface cleaning [1]. The use of inhibitors for the control of corrosion for metals and alloys which are in contact with aggressive environment is an accepted practice. Large numbers of organic compounds were studied to investigate their corrosion inhibition potential. All these studies reveal that organic compounds especially those with N, S and O showed significant inhibition efficiency [2-7]. Little work [8-14] appears to have been done on the inhibition of mild steel in phosphoric acid solutions. DFT (density functional theory) methods have become very popular in the last decade due to their accuracy and less time requirement from the computational point of view [15]. Based on the well-known Hohenberg-Kohn theorems [16], DFT focuses on the electron density, ρ(r), itself as the carrier of all information in the molecular (or atomic) ground state. Important molecular properties of molecules such as dipole moment, E_{HOMO}, E_{LUMO},ΔE_{L-H}, etc…, have been correlated with inhibition efficiency of different

inhibitors using DFT[17]. In this paper, the kinetics of the corrosion of carbon steel in phosphoric acid have been studied bypotentiodynamic polarization, electrochemical impedance spectroscopy, weightloss, methods and theoretical studies. The action of Sulfapyridine as inhibitor in phosphoric acid medium over a range of acid concentration and solution temperature has also been examined.

MATERIALS AND METHODS

Materials

The steel used in this study is a carbon steel (Euronorm: C35E carbon steel and US specification: SAE 1035) with a chemical composition (in wt%) of 0.370 % C, 0.230 % Si, 0.680 % Mn, 0.016 % S, 0.077 % Cr, 0.011 % Ti, 0.059 % Ni, 0.009 % Co, 0.160 % Cu and the remainder iron (Fe). The carbon steel samples were pre-treated prior to the experiments by grinding with emery paper SiC (120, 600 and 1200); rinsed with distilled water, degreased in acetone in an ultrasonic bath immersion for 5 min, washed again with bidistilled water and then dried at room temperature before use.

Solutions

The aggressive solutions of 2.0 M H_3PO_4 was prepared by dilution of analytical grade 85% H_3PO_4 with distilled water. The concentration range of Sulfapyridine used was 5×10^{-4}M to 1×10^{-5}M.

Corrosion tests

Weight loss

Gravimetric measurements were carried out at definite time interval of 6 h at room temperature using an analytical balance (precision ± 0.1 mg). The carbon steel specimens used have a rectangular form (length = 1.6 cm, width = 1.6 cm, thickness = 0.07 cm). Gravimetric experiments were carried out in a double glass cell equipped with a thermostated cooling condenser containing 80 mL of non-de-aerated test solution. After immersion period, the steel specimens were withdrawn, carefully rinsed with bidistilled water, ultrasonic cleaning in acetone, dried at room temperature and then weighed. Triplicate experiments were performed in each case and the mean value of the weight loss was calculated.

Electrochemical impedance spectroscopy

The electrochemical measurements were carried out using Volta lab (Tacussel- Radiometer PGZ 100) potentiostate and controlled by Tacussel corrosion analysis software model (Volta master 4) at under static condition. The corrosion cell used had three electrodes. The reference electrode was a saturated calomel electrode (SCE). A platinum electrode was used as auxiliary electrode of surface area of 1 cm^2. The working electrode was carbon steel. All potentials given in this study were referred to this reference electrode. The working electrode was immersed in test solution for 30 minutes to a establish steady state open circuit potential (E_{ocp}). After measuring the E_{ocp}, the electrochemical measurements were performed. All electrochemical tests have been performed in aerated solutions at 298 K. The EIS experiments were conducted in the frequency range with high limit of 100 kHz and different low limit 100 mHz at open circuit potential, with 10 points per decade, at the rest potential, after 30 min of acid immersion, by applying 10 mV ac voltage peak-to-peak. Nyquist plots were made from these experiments. The best semicircle can be fit through the data points in the Nyquist plot using a non-linear least square fit so as to give the intersections with the x-axis.

Potentiodynamic polarization

The electrochemical behaviour of carbon steel sample in inhibited and uninhibited solution was studied by recording anodic and cathodic potentiodynamic polarization curves. Measurements were performed in the 2.0 M H_3PO_4solution containing different concentrations of the tested inhibitor by changing the electrode potential automatically from - 800 to -200 mV versus corrosion potential at a scan rate of $2mV.s^{-1}$. The linear Tafel segments of anodic and cathodic curves were extrapolated to corrosion potential to obtain corrosion current densities (I_{corr}).

The present investigation was undertaken to examine the corrosion inhibition capacity of Sulfapyridinein 2.0 M H_3PO_4solution on carbon steel at 298-328 K using potentiodynamic polarisation (PDP) curves and electrochemical impedance spectroscopy (EIS) methods. The adsorption isotherm of inhibitor on steel surface was determined. Kinetic parameters are calculated and discussed in detail. Figure 1 shows the molecular structure of the Sulfapyridineutilised in this investigation.

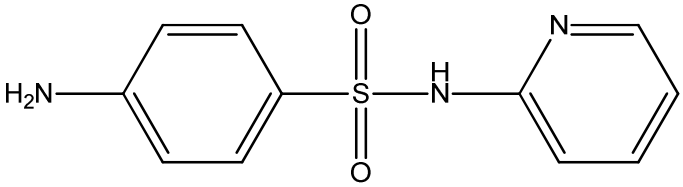

Figure 1: Chemical structure of Sulfapyridine

Computational procedures

Complete geometrical optimizations of the investigated molecules are performed using DFT (density functional theory) with the Beck's three parameter exchange functional along with the Lee-Yang-Parr nonlocal correlation functional (B3LYP) [18-20] with 6-31G(d) basis set is implemented in Gaussian 03 program package [21]. This approach is shown to yield favorable geometries for a wide variety of systems. This basis set gives good geometry optimizations. The geometry structure was optimized under no constraint. The following quantum chemical parameters were calculated from the obtained optimized structure: The highest occupied molecular orbital (E_{HOMO}) and the lowest unoccupied molecular orbital (E_{LUMO}), the energy difference (ΔE) between E_{HOMO} and E_{LUMO}, dipole moment (μ), electron affinity (E*A*), ionization potential (*I*) and the fraction of electrons transferred (ΔN).
Ionization potential (*I*) and electron affinity (*A*) are related [22] in turn to E_{HOMO} and E_{LUMO} as follows:

$I = -E_{HOMO}$
$A = -E_{LUMO}$

The absolute electronegativity χ and the absolute hardness η are related [23] in turn to I and A as follows:

$$\chi = \frac{I + A}{2} \quad (1)$$

$$\eta = \frac{I - A}{2} \quad (2)$$

The global electrophilicity index was introduced by Parr [24] and is given by:

$$\omega = \frac{\chi 2}{2\eta} \quad (3)$$

The number of transferred electrons (ΔN) was also calculated depending on the quantum chemical method [25, 26] by using the equation;

$$\Delta N = \frac{\chi_{Fe} - \chi_{inh}}{2(\eta_{Fe} + \eta_{inh})} \quad (4)$$

Where χ_{Fe} and χ_{inh} denote the absolute electronegativity of iron and inhibitor molecule η_{Fe} and η_{inh} denote the absolute hardness of iron and the inhibitor molecule respectively. In this study, we use the theoretical value of χ_{Fe} =7.0 eV and η_{Fe} = 0, for calculating the number of electron transferred.

RESULTS AND DISCUSSION

Effect of concentration inhibitor

Weight loss

The corrosion rate (A) of carbon steel specimens after 2 h exposure to 2.0 M H_3PO_4solution with and without the addition of various concentrations of the investigated inhibitor was calculated and the obtained data are listed in Table 1. The variation of A with inhibitor concentrations is shown in Fig. 2. The corrosion rate, A (mg cm^{-2} h^{-1}), surface coverage (θ) and inhibition efficiency η_w of each concentration were calculated using the following equations [27]:

$$A = \frac{\Delta W}{St} \quad (5)$$

$$\theta = \frac{A_{uninh} - A_{inh}}{A_{uninh}} \quad (6)$$

$$\eta_W = \left(\frac{A_{uninh} - A_{inh}}{A_{uninh}} \right) \times 100 \quad (7)$$

Where ΔW is the average weight loss (mg), S is the surface area of specimens (cm^2), and t is the immersion time (h), $A_{uninh}$and A_{inh} are corrosion rates in the absence and presence of inhibitor, respectively.

Table1. Effect ofSFP concentration on corrosion data of carbon steel in 2.0 M H_3PO_4

Inhibitor	Conc. (M)	A (mg cm^{-2} h^{-1})	η_w (%)	(θ)
Blank	2.0	1.972	-	-
SFP	5×10^{-4}	0.0722	96.34	0.9634
	1×10^{-4}	0.1631	91.73	0.9173
	5×10^{-5}	0.2321	88.23	0.8823
	1×10^{-5}	0.3557	81.96	0.8196

From the Table1 and the Fig.2, it is clear that increase of inhibitor concentration caused a decrease in the weight lossas well as corrosion rate of mild steel and, increasing the efficiency of inhibition to reach the maximum value of**96.34**% at the highest concentration of 5×10^{-4}M. This shows that the molecule of **SFP**may be adsorbed on the metalsurface to cover the active sites on the electrode surface.

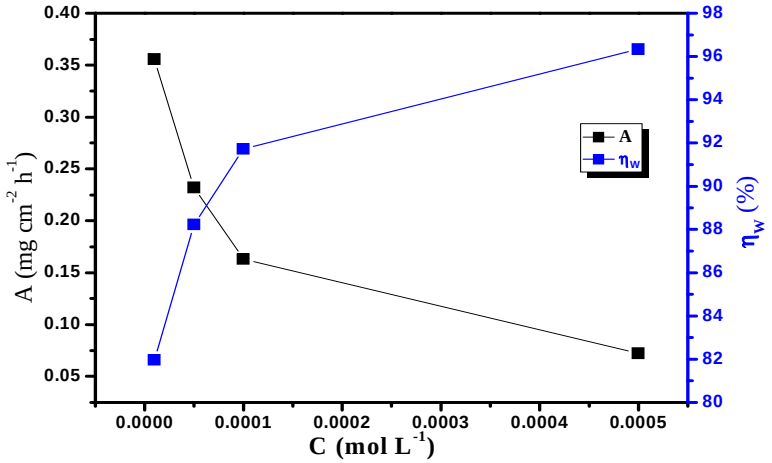

Figure 2.Variation of inhibition efficiency and corrosion rate in 2.0 M H_3PO_4 on mild steel surface without and with different concentrations of SFP

Electrochemical impedance spectroscopy

Nyquist representation of the EIS study of mild steel in 2.0 M H_3PO_4in absence and presence of different concentration of **SFP** were presented in figure 3. The large capacitive loop attributed to the adsorption of the inhibitor molecule [28]. The simple equivalent Randle circuit for studies is shown in Fig. 3, where Rs represents the solution and corrosion product film; the parallel combination of resister, R_{ct} and capacitor C_{dl} represents thecorroding interface. The existence of single semi circle showed the single charge transfer process. Depression fromthe perfect semi circle is due to the inhomogeneous nature of the metal surface arising from the surface roughness orthe interfacial phenomenon [29]. The increase in R_{ct} values due to the addition of inhibitor in comparison to the absence of inhibitor is attributed to the formation of protective film on the metal/solution interface. These observations suggest that **SFP** molecules function by adsorption at metal surface thereby causing the decrease in C_{dl} values and increase in R_{ct} values [30].

The electrochemical parameters, including R_{ct}, Y_0 and n, obtained from fitting the recorded EIS data using the electrochemical circuit of Figure 4 are listed in Table 2. The impedance of the CPE is expressed as follows [51].

$$Z_{CPE} = \frac{1}{Y_0 (j\omega)^n} \quad (8)$$

Where Y_0 is the CPE constant, n is the phase shift which can be explained as a degree of surface inhomogeneity, j is the imaginary unit and ω is the angular frequency. Depending on the values of n, CPE can represent resistance

(n=0), capacitance (n=1), inductance (n= -1) and Warburg impedance (n=0.5). The values of the interfacial capacitance C_{dl}can be calculated from CPE parameter values Y_0 and n using the expression [32]:

$$C_{dl} = \frac{Y_0 \omega^{n-1}}{\sin(n\pi/2)} \quad (9)$$

Decrease in C_{dl}, which can result from a decrease in local dielectric constant and/or an increase in the thickness of the electrical double layer, suggests that the inhibitor molecules act by adsorption at the metal/solution interface [33].

The R_{ct} values were used to calculate the inhibition efficiency, η_z(%), (listed in Table 2), using the following equation:

$$\eta_z\% = \frac{R_{ct}^{i} - R_{ct}^{\circ}}{R_{ct}^{i}} \times 100 \quad (10)$$

Where R_{ct}° and R_{ct}^{i} are the charge transfer resistance in absence and in presence of inhibitor, respectively.

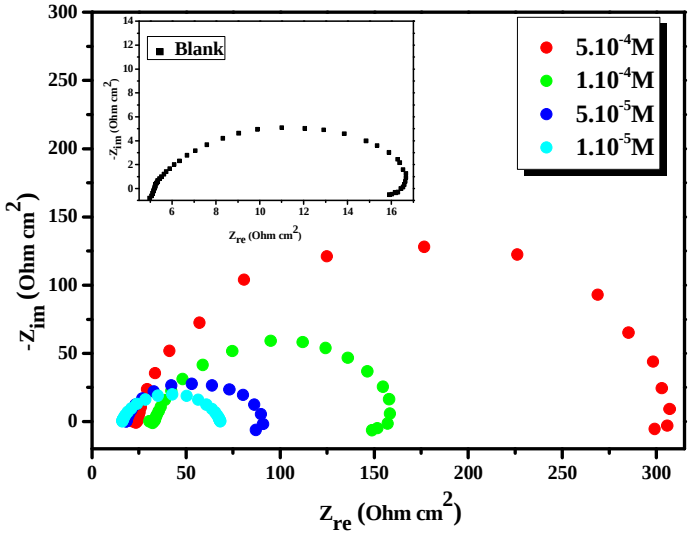

Figure3. Nyquist diagrams of carbon steel with different concentrations of SFP at 298K

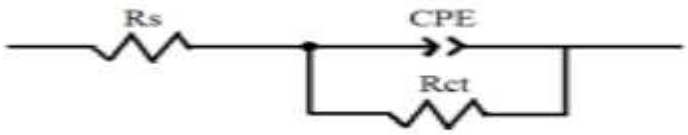

Figure4. Equivalent electrical circuit corresponding to the corrosion process on the carbon steel in phosphoric acid

Table2. Electrochemical Impedance parameters for corrosion of carbon steel in acid medium at various contents of SFP

Inhibitor	Concentration (M)	R_t (Ω cm^2)	$Y_0\times10^{-5}$ ($s^n\ \Omega^{-1}cm^{-2}$)	n	C_{dl} (μF/cm^2)	η_z (%)
Blank	2.0	14	21.024	0.88	94.96	—
SFP	5×10^{-4}	299.2	1.2542	0.92	07.72	94.8
	1×10^{-4}	149	3.0945	0.91	18.18	90.6
	5×10^{-5}	67.1	5.7878	0.88	27.15	79.1
	1×10^{-5}	52.3	9.5927	0.83	32.43	73.2

Polarization curves

The potentiodynamic polarization measurements were carried out to study the kinetics of the cathodic and anodic reactions. Figure 5 shows the results of the effect of Sulfapyridine inhibitor on the cathodic as well as anodic polarization curves of mild steel in 2.0 M H_3PO_4respectively. It is evident from the figure that both reactions were suppressed with the addition of this inhibitor. This suggests that Sulfapyridine reduced the anodic dissolution reactions as well as retarded the hydrogen evolution reactions on the cathodic sites. Electrochemical corrosion kinetic parameters namely corrosion potential (E_{corr}), corrosion current density (I_{corr}) and cathodic Tafelslope (βc) obtained from the extrapolation of the polarization curves are listed in Table 3.

The I_{corr} values were used to calculate the inhibition efficiency, η_{IE}(%), (listed in Table 3), using the following equation [34]:

$$\eta_{IE}\% = \frac{I_{corr} - I_{corr(i)}}{I_{corr}} \times 100 \qquad (11)$$

Where, I_{corr} and $I_{corr(i)}$ are the corrosion current density in absence and presence of inhibitor, respectively.

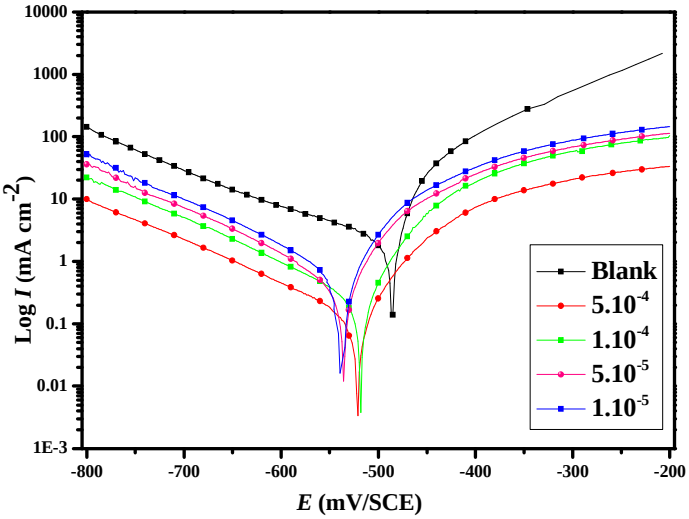

Figure5. Potentiodynamic polarization curves of carbon steel in 2.0 M H_3PO_4 in the presence of different concentrations of SFP

E_{corr} values was shifted towards less negative potential which is a necessary to quote the inhibitive action of inhibitor and to classify an inhibitor into an anodic, a cathodic, or mixed type. It has been reported that [35], an inhibitor can be classified as an anodic or a cathodic-type inhibitor on the basis of magnitude of shift in E_{corr} value. If displacement in E_{corr} is greater than 85 mV, towards anode or cathode with reference to blank, then an inhibitor is categorized as either anodic or cathodic type inhibitor, respectively. Otherwise an inhibitor is treated as mixed type. In our study, maximum displacement in E_{corr} value was around 64 mV indicating Sulfapyridine area mixed type inhibitor, in 2.0 M H_3PO_4. Fig. 5 represents the polarisation curves of C38 steel in 2.0 M H_3PO_4without and with the different inhibitors in concentrations of 5 $\times 10^{-4}$M -1 $\times 10^{-5}$Mby weight at 298 K. It is clear from Fig. 5that the cathodic current densities decrease with increasing the concentrations of the inhibitors; this indicates that these compounds are adsorbed on the metal surface and hence inhibition occurs. Thus, the addition of this inhibitor hindered the acid attack on the C38 steel electrode. The parallel cathodicTafel curves in Fig. 5 reveal that the hydrogen evolution is activation–controlled and the hydrogen evolution reaction (reduction mechanism) is not affected by the presence of the inhibitors [36].

Table3. Electrochemical parameters of carbon steel at various concentrations of SFP in 2.0 M $H_3PO_4$and corresponding inhibition efficiency

Inhibitor	Concentration (M)	E_{corr} vs. SCE (mV)	$-\beta_c$ (mV dec^{-1})	I_{corr} (µA cm^{-2})	η_{Tafel} (%)
Blank	2.0	-488	135	2718	—
(SFP)	5×10^{-4}	-526	139	125	95.4
	1×10^{-4}	-541	136	241	91.2
	5×10^{-5}	-548	142	483	82.3
	1×10^{-5}	-552	149	618	77.3

The results in Table 3 show that the inhibition efficiency increased, while the corrosion current density decreased with the addition of inhibitors. This may be due to the adsorption of inhibitors on C38 steel/acid interface. The lowest current density value (125µA cm^{-2}) and best inhibition efficiency was obtained for **SFP** at 5×10^{-4}. The results in Table 3 indicated that the increase of inhibition efficiency with concentration might be attributed to the formation of the barrier film which prevented acid medium from attacking the metal surface.

Effect of temperature

Being given that the temperature is one of the factors that may affect the behavior of a material in a corrosive environment, and can also modify the metal-inhibitor interaction, it is essential to study the effect of this factor on the protection rates, as well to determine the mechanism of inhibition, that for calculating the activation energies of the corrosion process.

The study of the influence of temperature on the rate of corrosion inhibition of C38 steel by our inhibitor were performed at temperatures 298, 308, 318, and 328K in the absence and in the presence of inhibitor at 5×10^{-4}M for 0.5h immersion by potentiodynamic polarization (Figs.6 and 7).

The inhibition efficiencies are found to decrease with increasing the solution temperature from 298K to328 K. This behaviour can be interpreted on the basis that the increase in temperature results in desorption of the inhibitor molecules from the surface of carbon steel. Table 4 shows that the current densities increased with increasing temperature both in uninhibited and inhibited solutions. The current density increases more rapidly with temperature in the absence of the inhibitor. These results confirm that Sulfapyridine acts as an efficient inhibitor for carbon steel in 2.0 M H_3PO_4in the range of temperature studied.

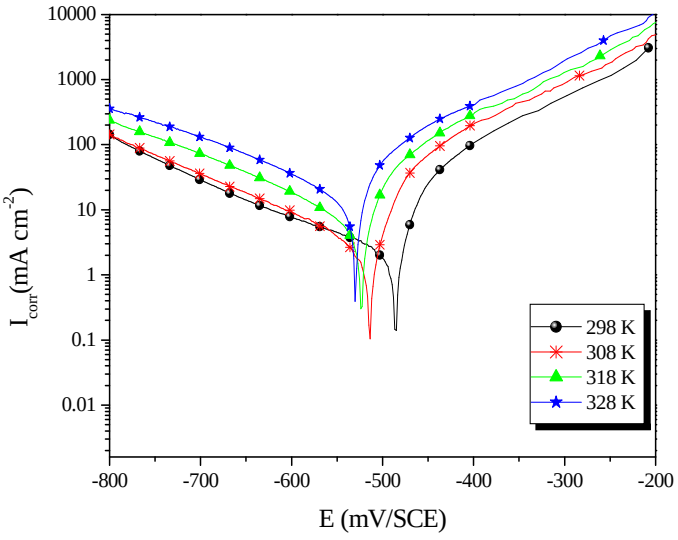

Figure6. Potentiodynamic polarisation curves of carbon steel in 2.0M H_3PO_4 at different temperatures

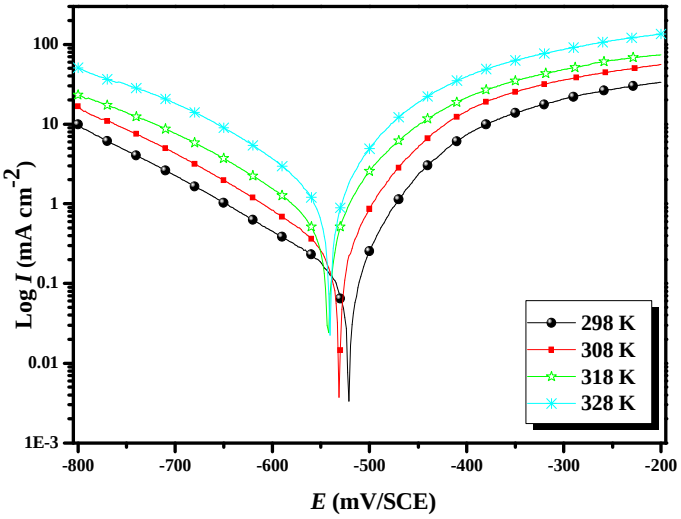

Figure7.Potentiodynamic polarization curves of carbon steel in 2M H_3PO_4 in the presence5×10^{-4}M of SFP at different temperatures

Table4. Various corrosion parameters for carbon steel in 2M H_3PO_4 in absence and presence of optimum concentration of SFP at different temperatures

Inhibitor	Temperature K	E_{corr} vs. SCE(mV)	$-\beta_c$ (mV dec^{-1})	i_{corr} (µA cm^{-2})	η_{Tafel} (%)
Blank	298	-488	135	2718	—
	308	-532	137	4220	—
	318	-523	132	6610	—
	328	-514	139	11890	—
5×10^{-4}M (SFP)	298	-526	139	125	95.4
	308	-537	146	308	92.7
	318	-548	143	648	90.2
	328	-546	146	1593	86.6

The activation parameters were calculated from the Arrhenius-type plot according to equation:

$$I_{corr} = k\exp\left(-\frac{E_a}{RT}\right) \quad (12)$$

Where E_a is the apparent activation corrosion energy, R is the universal gas constant and k is the Arrhenius pre-exponential constant.

Arrhenius plots for the corrosion density of carbon steel in the case of **SFP** are given in Fig. 8. Values of apparent activation energy of corrosion (E_a) for carbon steel in 2.0 M H_3PO_4 with the absence and presence of Sulfapyridine were determined from the slope of Ln (I_{corr}) versus 1/T plots and shown in Table 5.

According to the report in literature [37, 38], higher value of E_a was considered as physical adsorption that occurred in the first stage. Because the electrochemical corrosion is relevant to heterogeneous reactions, the preexponential factor A in the Arrhenius equation is related to the number of active centers. There are two possibilities about these active centers with different E_a on the metal surface: (1) the activation energy in the presence of inhibitors is lower than that of pure acidic medium, namely E_a(-inh) <E_a(H_3PO_4), which suggests a smaller number of more active sites remain uncovered in the corrosion process; (2) the activation energy in the presence of inhibitor is higher than that of pure acidic medium, E_a(inh) >E_a(H_3PO_4), which represents the inhibitor adsorbed on most active adsorption sites (having the lowest energy) and the corrosion takes place chiefly on the active sites (having higher energy).

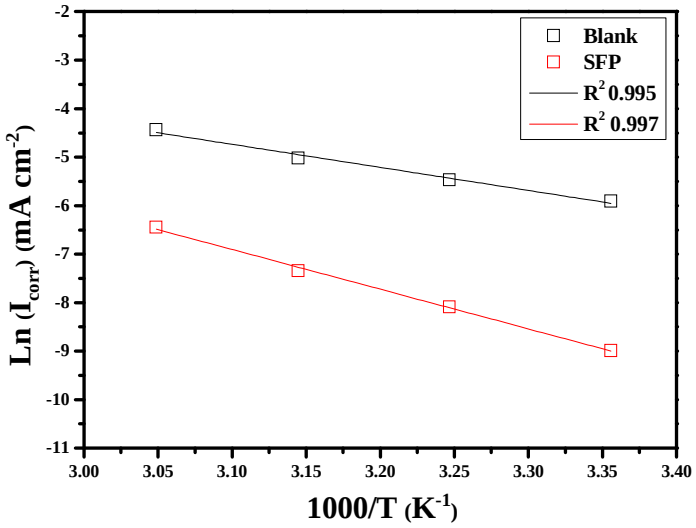

Figure8. Arrhenius plots of carbon steel in 2.0 M H_3PO_4 with and without 5×10^{-4}M of SFP

Activation parameters like enthalpy (ΔH_a) and entropy (ΔS_a) for the dissolution of carbon steel in 2.0 M H_3PO_4in the absence and presence of 5×10^{-4}M**SFP** were calculated from the transition state equation:

$$i_{corr} = \frac{RT}{Nh}\exp\left(\frac{\Delta S_a}{R}\right)\exp\left(-\frac{\Delta H_a}{RT}\right) \qquad (13)$$

Where h is Planck's constant, N is the Avogadro number, R is the universal gas constant, ΔH_a is the enthalpy of activation and ΔS_a is the entropy of activation.

Fig. 9 shows that the Arrhenius plots of Ln (i_{corr}/T) versus 1/T gave straight lines with slope ($-\Delta H_a$/R) and intercept (Ln R/Nh + ΔS_a/R) from where ΔH_a and ΔS_a values were calculated. The activation parameters are given in Table 5.

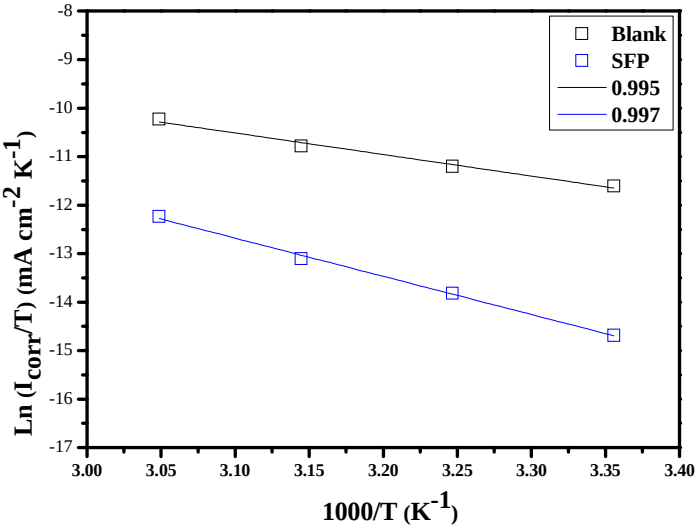

Figure9. Arrhenius plots of carbon steel in 2.0 M H_3PO_4 with and without 5×10^{-4}M of SFP

Table5. The values of activation parameters E_a, ΔH_a and ΔS_a for carbon steel in 2.0 M H_3PO_4 in the absence and presence of 5×10^{-4}M of SFP

Concentration (M)	E_a (kJ mol^{-1})	ΔH_a (kJ mol^{-1})	ΔS_a (J mol^{-1} K^{-1})	E_a-ΔH_a (kJ mol^{-1})
Blank	39.50	36.91	-112.98	2.59
5×10^{-4}M **SFP**	68.05	65.45	-100.06	2.60

In this study he values of E_a obtained from the slopes of these straight lines are recorded in Table 5. The values of E_a were higher for inhibited solutions indicating physical adsorption of the inhibitor on the metal surface [39, 40]. However, this energy increases with the addition of the Sulfapyridine compounds into molar solution of phosphoric acid, which shows a change in the mechanism of transition metal in solution. However, several authors [47-46] showed that the increase in Ea may often be interpreted by the formation of an adsorption film by a physical mechanism (electrostatic). The values of E_a and ΔH_a were increased in the presence of inhibitors, suggesting that the energy barrier of the corrosion reaction increases, meaning that the dissolution of the steel is difficult [44]. According Gomma et al [45], the activation energy is much higher than the inhibitor is more effective. However, the positive sign of the endothermic enthalpy reflects the nature of the dissolution of the steel. We note that the variation of the activation energy E_a and the enthalpy of ΔH_a vary in the same way with the concentration of inhibitor, which satisfies the relationship between E_a and thermodynamics as ΔH_a [47]: $E_a - \Delta H_a = RT$. The large negative values of entropies (ΔS_a)from **SFP** imply that the activated complex in the rate determining step represents an association rather than a dissociation step, meaning that a decrease in disordering takes place on going from reactants to the activated complex [48].

Adsorption isotherm and standard adsorption free energy

The inhibition of corrosion of metals by organic compounds is explained by their adsorption. The latter is described by two main types of adsorption, namely physical adsorption and chemical adsorption. It depends on the charge of the metal, the nature of the chemical structure of the organic product and the type of electrolyte. The presence of a transition metal, having orbital "d" vacant, and a molecule having centers that facilitates electron rich adsorption [49,50].

The adsorption isotherm can be determined if the mode of action of the inhibitor is mainly due to adsorption on the metal surface. And the type of these isotherms can provide additional information regarding the inhibitory properties of the compounds tested. However, if we assume that the adsorption of our inhibitors adsorption isotherm follows Langmuir, the rate of surface coverage (θ) for different concentrations in acidic medium is evaluated by the method of weight loss according to the report E_w (%) / 100 and using the following equation [51]:

$$\frac{C_{inh}}{\theta} = \frac{1}{K_{ads}} + C_{inh} \qquad (14)$$

Where C_{inh} is the concentration of inhibitor and K_{ads} the adsorptive equilibrium constant.

Figure 10 shows the curves of the variation of C_{inh} / θ according to the concentration C_{inh} for the Sulfapyridine compound. The linearity of these curves indicates that the adsorption of our inhibitors on the surface of C38 steel in 2.0 M H_3PO_4, is according to the Langmuir isotherm model checking equation (14). The validity of this approach is confirmed by the strong correlation (R^2= 0.999 for the compound **SFP**).

The values of K_{ads} obtained from the reciprocal of intercept of Langmuir isotherm line are listed in Table 6, together with the values of the Gibbs free energy of adsorption ΔG°_{ads} calculated from the equation:

$$K_{ads} = (\frac{1}{55.5}) \exp(-\frac{\Delta G^{\circ}_{ads}}{RT}) \qquad (15)$$

Where R is gas constant and T is absolute temperature of experiment and the constant value of 55.5 is the concentration of water in solution in mol dm^{-3}.

The high values of adsorption equilibrium constants K_{ads} correspondent's Sulfapyridine compound to reflect the high adsorption capacity of these inhibitors on the surface of C38 steel in acidic 2.0 M H_3PO_4. This suggests that this inhibitor can best recoveries, where it's most effective protection against corrosion.

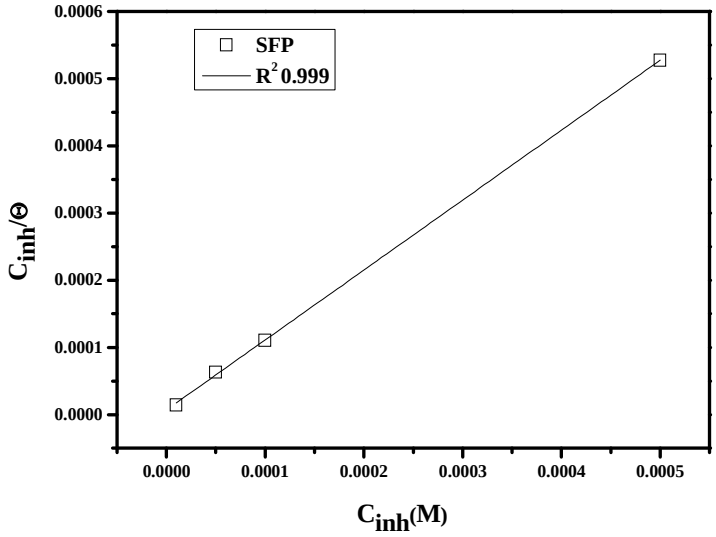

Figure10. Adsorption isotherm according to Langmuir's model derived from EIS measurement

Table5. Thermodynamic parameters for the adsorption of SFP in 2.0 M H_3PO_4on the carbon steel at 298K.

Inhibitor	Slope	$K_{ads}(M^{-1})$	$\Delta G°_{ads}$(kJ/mol)
SFP	1.04	142603.51	**39.35**

The negative values of the standard free energy of adsorption indicates a spontaneous adsorption of molecules on the surface of our C38 steel and also the strong interaction between the inhibitors molecules and the metal surface [52,53]. In general, the standard values of free energy of-20 kJ mol^{-1} or less negative are associated with an electrostatic interaction between the charged molecules and charged metal surface (physical adsorption), those from-40 kJ mol^{-1} or more negative involves a load sharing or transfer inhibitor molecules to the metal surface to form a coordinate covalent bond (chemisorption) [54-56]. The values of $\Delta G°_{ads}$ in our measurements (in Table 4) is -39.35kJ $mol^{-1}$for **SFP**, it is suggested that the adsorption of this **SFP** involves two types of interactions: chemisorption and physisorption [57].

Theoretical parameters predicating

Quantum chemical methods and molecular modeling techniques enable the definition of a large number of molecular quantities characterizing the reactivity, shape, and binding properties of a complete molecule as well as of molecular fragments and substituent's. The geometry of the inhibitor as well as the nature of its frontier molecular orbitals, namely, the HOMO and LUMO is involved in the activity properties of the inhibitors. Therefore, in this study, quantum chemical calculations were performed to investigate the relationship between molecular structure of this compound and their inhibition effect. The optimized molecular structure and the frontier molecule orbital density distribution of the studied molecule are shown in Fig. 11, and the calculated quantum chemical parameters E_{HOMO}, E_{LUMO}, ΔE (E_{LUMO} - E_{HOMO}), dipole moment (μ), number of transferred electrons (ΔN), and total energy (TE) are given in Table 6.

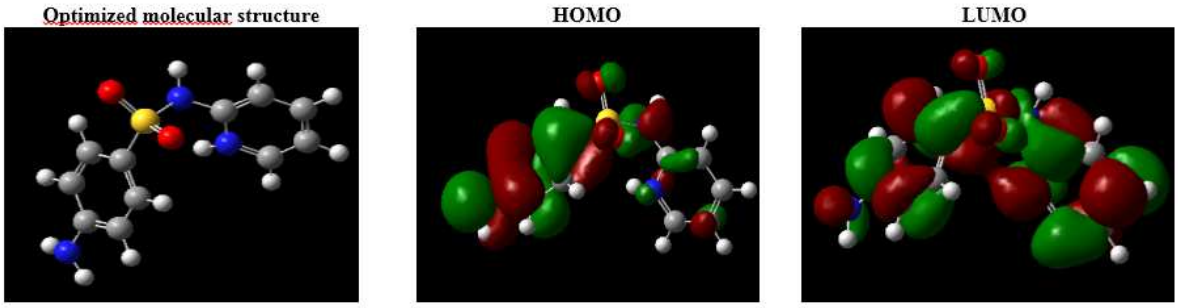

Figure 11. The optimized molecular structure and frontier molecular orbital density distributions of SFP

Table 6. Quantum chemical parameters for SFP calculated using B3LYP/6-31G (d,p)

Molecular parameters	**SFP**
E_{HOMO} (eV)	-3.3567983
E_{LUMO} (eV)	-0.94505192
ΔE_{gap} (eV)	2.41174638
μ (debye)	7.5398
I (eV)	3.3567983
A (eV)	0.94505192
χ (eV)	2.15092511
η (eV)	1.20587319
ω	2.7894734
ΔN	2.0106073
TE (a.u)	-1139.39

Frontier orbital theory is useful in predicting adsorption centers of the inhibitor molecules responsible for the interaction with surface metal atoms [58, 59]. Terms involving the frontier MO could provide dominative contribution, because of the inverse dependence of stabilization energy on orbital energy difference [58]. It has been reported in the literature that the higher the HOMO energy of the inhibitor, the greater the trend of offering electrons to unoccupied d orbital of the metal, and the higher the corrosion inhibition efficiency. In addition, the lower the LUMO energy, the easier the acceptance of electrons from metal surface, as the LUMO–HOMO energy gap decreased and the efficiency of inhibitor improved [60]. For the dipole moment (μ), higher value (7.5398D) will favor a strong interaction of inhibitor molecules to the metal surface. The number of transferred electrons depends strongly on what the actual quantum chemical method employed for computation. Furthermore, the expression ‘‘number of transferred electrons’’ is the wording ‘‘electron-donating ability’’, which does not imply that the figures of ΔN actually indicate the number of electrons leaving the donor and entering the acceptor molecule. The value of electron-donating ability (ΔN) was calculated and its value is given in **Table 6**. If ΔN < 3.6 (electron), the inhibition efficiency increases with increasing value of ΔN, while it decreased if ΔN > 3.6 (electron) [61]. In present contribution, **SFP** is the donor of electrons, and the iron surface atom was the acceptor. The **SFP** was bound to the mild steel surface, and thus formed inhibition adsorption layer against corrosion at carbon steel/hydrochloric acid solution interface.

CONCLUSION

All the measurements showed that the **SFP** has excellent inhibition properties against the mild steel corrosion in phosphoric acid solution. Inhibition efficiency of this inhibitor decreases with increase in temperature and further it leads to an increase in activation energy. The inhibitor follows the Langmuir adsorption isotherm in the process of adsorption. EIS measurements also indicates that the inhibitor performance increase due to the adsorption of molecule on the metal surface. Potentiodynamic polarization measurements showed that the inhibitor acts as mixed type of inhibitor. The inhibitor showed maximum inhibition efficiency at 5×10^{-4}M concentration of the studied inhibitor. The inhibition efficiencies determined by EIS, potentiodynamic polarization and weight loss studies are in good agreement. Theoretical calculations provide good support to experimental results.

Acknowledgment
The authors would like to thank the Palestenian Ministry of Higher Education for their support.The support given through an “INCRECYT” research contract to M. Zougagh is also acknowledged.

REFERENCES

[1] Schmitt G, Brit,*Corros. J*,**1984**, 19, 165.
[2] M Larouj, M Belayachi, H Zarrok, A Zarrouk, A Guenbour, M EbnTouhami, AShaim, S Boukhriss, H Oudda, B Hammouti, ,**2014**, 6, 373-384
[3]MLarouj, Y ELaoufir, H Serrar, A El Assyry, M Galai, A Zarrouk, B Hammouti, A Guenbour, AElMidaoui, S Boukhriss, M EbnTouhami and HOudda,*Der Pharmacia Lettre*,**2014**, 6, 324-334.
[4] M Larouj, H Lgaz, H Zarrok, H Serrar, H Zarrok, H Bourazmi, A Zarrouk, A Elmidaoui, AGuenbour, S Boukhris and H Oudda,*Journal of Material and Environmental Science*,**2015**, 6, 3251-3267.
[5]M Larouj, MBelkhaouda, H Lgaz, R Salghi, S Jodeh, S Samhan, H Serrar, S Boukhris, M Zougagh and H Oudda,*Der PharmaChemica*,**2016**, 8, 114-133.
[6] H Lgaz, O Benali, R Salghi, S Jodeh, M Larouj, O Hamed, M Messali, S Samhan, M Zougagh and H Oudda,*Der PharmaChemica*,**2016**, 8, 172-190.
[7] L Afia, M Larouj, H Lgaz, R Salghi, S Jodeh, S Samhan and M Zougagh,*Der PharmaChemica*,**2016**, 8, 22- 35.
[8] Khamis E, Ameer M A, Alandis N M, AL-Senani G, *Corrosion*, **2000**, 56, 2, 127.

[9] MalkiAlaoui L, Hammouti B, Bellaouchou A, Benbachir A, Guenbour A, Kertit S, Der *Pharm. Chem*,**2011**, 3 ,353.
[10] Abu Al-Ola KA A, Al-Nami S Y, Mod. *Appl. Sci*,**2011**, 5, 193.
[11] Benabdellah M, Touzani R, Dafali A, Hammouti B, El Kadiri S,*Mater. Lett*,**2007,**61, 1197.
[12] Benabdellah M, Aouniti A, Dafali A, Hammouti B, Benkaddour M, Yahyi A, Ettouhami A,*Appl. Surf. Sci*,**2006**, 252, 8341.
[13] Li X, Deng S, Fu H,*Corros. Sci*,**2012**, 55, 280.
[14] Wang L, Yin G Y, Zhang Q F, Pu J X, *Corrosion*,**2000**, 56, 1083.
[15] K F Khaled, M A Amin,*Corros. Sci*,**2009,** 2098.
[16] Hohenberg P, Kohn W,*Phys. Rev.A*,**1964**,136, 864.
[17] Wang H, Wang X, Wang H, Wang L, Liu A,*J. Mol. Model*,**2007**, 13, 147.
[18] A D Becke, J. *Chem. Phy*,**1992**, 96, 9489.
[19] A DBecke, *J. Chem. Phy*,**1993**, 98, 1372.
[20] C Lee, W Yang, R G Parr,*Phy. Rev*,*B*,**1988**, 37, 785.
[21] M J Frisch et al Gaussian 03, Revision C.02, Gaussian Inc, Pittsburgh, PA, **2003**.
[22] M J S Dewar, W Thiel, *J. Am. Chem. Soc*, **1977**, 99, 4899.
[23] R G Pearson,*Inorg. Chem.***1988**, 27, 734.
[24] V S Sastri, J R Perumareddi,*Corrosion*, **1997**, 53, 671
[25] V S Sastri, J R Perumareddi,*Corrosion (NACE).***1997**, 53, 617.
[26] I Lukovits, E Kalman, F Zucchi,*Corrosion (NACE)*,**2001**, 57, 3.
[27] W Chen, H Q Luo, N B Li,*Corros. Sc*,**2011**, 53, 3356.
[28] S K Shukla, M A Quraishi,*Corros. Sci*,**2010**, 52, 314.
[29] S K Shukla, M A Quraishi,*Corros. Sci*,**2009**,51, 1990.
[30] F Bentiss, MTraisnel, M Lagrenee,*Corros. Sci*,**2000**, 42, 127.
[31] Xingwen Zheng, Shengtao Zhang, Wenpo Li, Linliang Yin, Jiahong He, JinfangWua.*Corros. Sci*,**2014**, 80, 383-392.
[32] I B Obot, N O Obi-Egbedi, *Curr.Appl. Phys*,**2011**, 11, 382.
[33] GBereket, A Yurt,*Corros. Sci*,**2001**, 43, 1179.
[34] M Larif, A Elmidaoui, A Zarrouk, H Zarrok, R Salghi, B Hammouti, HOudda, F Bentiss,*Res. Chem. Intermed*, **2012**, DOI: 10.1007/s11164-012-0788-2.
[35] IshtiaqueAhamad,Rajendra Prasad, M AQuraishi,*Corros. Sci*,**2010**, 52, 1472.
[36] M A Hegazy, H M Ahmed, A SEl-Tabie,*Corros. Sci*,**2011**, 53, 671.
[37] S SAbd El-Rehim, M A M Ibrahim, K F Khaled,J. Appl. Electrochem,**1999**, 29, 593.
[38] S Martinez, I Stern, Appl. *Surf. Sci*,**2002**, 199, 83.
[39] H Zarrok, K Al Mamari, A Zarrouk, R Salghi, BHammouti, S S Al-Deyab, E MEssassi, F Bentiss, H Oudda,*Int. J. Electrochem. Sci*,**2012**, 7, 10338.
[40] F Bentiss, MLebrini, M Lagrenée,*Corros. Sc*,**2005**, 47, 2915.
[41] E EFoad El Sherbini,*Mat. Chem. Phys*,**1999**, 60, 286.
[42] K F Khaled, A El-mghraby, O B Ibrahim, O AElhabib, A M Magdy Ibrahim,*J. Mater. Environ. Sci*,**2010**, 1, 139.
[43] N P Clark, EJakson, M Robinson, Br. *Corros. J*,**1979**, 14, 33.
[44] TSzauer, A Brand,*Electrochim. Acta*,**1981**, 26, 1219.
[45] G K Gomma, M H Wahdan, *Mater. Chem. Phys*,**1995**, 39, 209.
[46] N M Guan, L Xueming and L Fei,*Mater. Chem. Phys*,**2004**, 86, 59.
[47] M Stern, A LGeary,*J. Electrochem. Soc*,**1957**, 104, 56.
[48] H Keles, M Keles, IDehri, O Serindag,*Mater. Chem. Phys*,**2008**, 112, 173.
[49]A HMehaute, G Grepy,*Solid State Ionics*,**1989**, 9, 17.
[50] K B Samardzija, C Lupu, NHackerman,A R Barron, *J. Mater. Chem*,**2005**, 15, 1908.
[51] I Langmuir,*J. Am. Chem. Soc*,**1917**, 39, 1848.
[52] I El Ouali, B Hammouti, A Aouniti, Y Ramli, MAzougagh, E M Essassi, M Bouachrine,*J. Mater. Environ. Sci*,**2010**, 1, 1.
[53] G Avci, *Mater. Chem. Phys*,**2008**, 112, 234.
[54] V Bransoi, M Baibarac, FBransoi, Internationnal. Cong. *Chemical Engineering, Romania*, **2001**, 215
[55] E Bayol, AAGurten, M Dursun, KKayakırılmaz,*Acta Phys. Chim. Sin*,**2008**, 24, 2236.
[56] O K Abiola, N C Oforka,*Mater. Chem. Phys*, **2004**, 83, 315.
[57] M Ozcan, R Solmaz, G Kardas, I Dehri,*Colloid Surf. A*,**2008**, 325, 57.
[58] H J Guadalupe, E Garcia-Ochoa, P J Maldonado-Rivas, J Cruz, T Pandiyan,*J. Electroanal. Chem*, **2011**.
[59] G Gece,*Corros. Sci*,**2008**, 50, 2981.
[60] F Bentiss, M Traisnel,*J. Appl. Electrochem*,**2001**, 31, 41.
[61] I Lukovits, E Kalman, F Zucchi,*Corrosion*,**2001**, 57, 3.